Heterodimerization of Endothelin-converting Enzyme-1 Isoforms Regulates the Subcellular Distribution of This Metalloprotease

Alain Barret, Eric Etienne, Rina Meidan, Olivier Valdenaire, Pierre Corvol, Claude Tougard, Laurent Muller

THE JOURNAL OF BIOLOGICAL CHEMISTRY
Vol. 278, No. 1, Issue of January 3, pp. 545–555, 2003
Printed in U.S.A.

Heterodimerization of Endothelin-converting Enzyme-1 Isoforms Regulates the Subcellular Distribution of This Metalloprotease*

Received for publication, September 3, 2002
Published, JBC Papers in Press, October 21, 2002, DOI 10.1074/jbc.M208949200

Laurent Muller‡, Alain Barret, Eric Etienne, Rina Meidan§, Olivier Valdenaire¶, Pierre Corvol, and Claude Tougard

From the INSERM U 36 Collège de France Paris, 75005 Paris, France

Endothelin-converting enzyme (ECE) is a membrane metalloprotease that generates endothelin from its direct precursor big endothelin. Four isoforms of ECE-1 are produced from a single gene through the use of alternate promoters. These isoforms share the same extracellular catalytic domain and contain unique cytosolic tails, which results in their specific subcellular targeting. We investigated the distribution of ECE-1 isoforms in transfected AtT-20 neuroendocrine cells. Whereas ECE-1a and 1c were present at the plasma membrane, ECE-1b and ECE-1d were retained inside the cells. We found that both intracellular isoforms were concentrated in the endosomal system: ECE-1d in recycling endosomes, and ECE-1b in late endosomes/multivesicular bodies. Leucine-based motifs were involved in the intracellular retention of these isoforms, and the targeting of ECE-1b to the degradation pathway required an additional signal in the N terminus. The concentration of ECE-1 isoforms in the endosomal system suggested new functions for these enzymes. Potential novel functions include redistribution of other isoforms through direct interaction. We have showed that ECE-1 isoforms could heterodimerize, and that in such heterodimers the ECE-1b targeting signal was dominant. Interaction of a plasma membrane isoform with ECE-1b resulted in its intracellular localization and decreased its extracellular activity. These data demonstrated that the targeting signals specific for ECE-1b constitute a regulatory domain *per se* that could modulate the localization and the activity of other isoforms.

Endothelins (ET[1]-1, ET-2, and ET-3) are 21-residue peptides derived from three distinct genes (1). They are pleiotropic factors that play an important role in the regulation of the cardiovascular and endocrine systems (for review see Refs. 2 and 3). Endothelins are also crucial developmental factors as demonstrated by the targeted disruption of the genes coding for the precursors of ET-1 and ET-3, and of the genes coding for their receptors, ETA and ETB (4–7). In addition, the expression of endothelin is associated with many pathological processes and with tumor growth (2, 8–10). In order to fulfill such a wide spectrum of physiological functions, endothelins act through autocrine and paracrine mechanisms. Their biosynthesis thus requires tight local control. Endothelins are synthesized in the endoplasmic reticulum as precursors that undergo a two-step proteolytic maturation. Pro-endothelins are first processed at conserved multibasic sites by furin or a furin-like enzyme, in order to release an intermediate called big endothelin (big-ET) (11, 12), which is devoid of biological activity (13). Big-ET is then processed by endothelin converting enzyme (ECE) at a Trp-Val/Ile bond, which releases the biologically active peptide. This latter proteolytic step can occur in the extracellular medium and in the secretory pathway, so that cells secrete either big-ETs alone or together with endothelins (14, 15, 16). Endothelial cells co-express the precursor, the converting enzyme and the receptor, thus implying autocrine function of endothelin. On the other hand, luteal cells (17) and neurons (18) express only the converting enzyme and the receptor, and three different cell types express the precursor, the converting enzyme and the receptor in seminiferous tubules (19), demonstrating the paracrine function of endothelin through extracellular processing of big-ET. The cellular distribution of ECE thus plays a central role in controlling the biosynthetic pathway of endothelins.

ECE is a type II membrane protein of the neutral endopeptidase (NEP) family, with an N-terminal cytosolic tail and a catalytic ectodomain. Unlike other proteases of this family, ECE is expressed as covalent dimers (20–22). Two genes coding for ECE-1 and ECE-2 have been cloned (20, 23, 14, 24). ECE-1 has a broader tissue distribution and is always expressed at higher levels than ECE-2. The targeted disruption of the ECE-1 gene resulted in a lethal phenotype that combined both the phenotypes of the inactivation of ET-1 or ETA and of ET-3 or ETB, thus demonstrating the central role of ECE-1 in the endothelin system (25). On the other hand, the inactivation of the ECE-2 gene did not result in significant modification of the mouse phenotype unless it was combined with the ECE-1 gene inactivation (26). ECE-1 is expressed in the endothelium of all organs as well as in nonvascular cells of many tissues including brain and neuroendocrine tissues (Refs. 14, 21, 18, and 27; for review see Ref. 28). Four isoforms of ECE-1 have been identified (Refs. 29 and 30; for review see Ref. 31), and a related gene organization has recently been described for ECE-2 (32, 33). ECE-1 isoforms result from the use of alternate promoters located upstream of specific exons (29, 30, 34). Thus, the 4 ECE-1 isoforms share the same catalytic domain and only differ in their N terminus, which codes for their cytosolic tails

* The costs of publication of this article were defrayed in part by the payment of page charges. This article must therefore be hereby marked "*advertisement*" in accordance with 18 U.S.C. Section 1734 solely to indicate this fact.

‡ To whom correspondence should be addressed: INSERM U36, Collège de France, 11 Place M.Berthelot, 75005 Paris, France. Tel: 33-1-44-27-14-29; Fax: 33-1-44-27-16-91; E-mail: laurent.muller@college-de-france.fr.

§ Present address: Dept. of Animal Science, Faculty of Agricultural, Food and Environmental Quality Sciences, The Hebrew University of Jerusalem, Rehovot 76100, Israel.

¶ Present address: AXOVAN AG, Gewerbestrasse 16, 4123 Allschwil, Switzerland.

[1] The abbreviations used are: ET, endothelin; ACTH, adrenocorticotropic hormone; Big-ET, big endothelin; ECE, endothelin-converting enzyme; NEP, neutral endopeptidase; TGN, *trans*-Golgi network; PBS, phosphate-buffered saline; DMEM, Dulbecco's modified Eagle's medium; PIPES, 1,4-piperazinediethanesulfonic acid.

(Fig.1*A*). As these domains are responsible for their targeting, the specificity of ECE isoforms resides in their subcellular distribution. Considering the importance of the intracellular and extracellular biosynthesis of endothelins, the subcellular distribution of ECE isoforms may play a central role in the regulation of the endothelin system and constitutes an important factor for the efficient inhibition of ECE in pathological conditions.

Extensive work aimed to define the intracellular localization of ECE-1 has been done in endothelial cells (21, 35, 36). Most of these studies were however non relevant to isoform specificity due to the lack of antibodies that can distinguish between ECE-1b, 1c, and 1d. More recent work was based on the expression of ECE-1 isoforms in transfected fibroblasts or epithelial cells. In these models, ECE-1a and ECE-1c were targeted to the plasma membrane, whereas ECE-1b was localized to intracellular organelles, and ECE-1d displayed an intermediate distribution (30, 37–39). Neuroendocrine cells constitute another major cell type expressing ECE-1 *in vivo* (28, 27). In these cells, precursors and peptides, as well as processing enzymes, are sorted between the constitutive and the regulated secretory pathways. We used the neuroendocrine AtT-20 cells as a model. These are corticotrope pituitary cells that are specialized in the synthesis and regulated secretion of adrenocorticotropic hormone (ACTH). In these cells, we investigated the subcellular distribution and the heterodimerization of ECE-1 isoforms, as the function of intracellular ECE-1 is a matter of debate, and the role of dimerization is still unknown.

MATERIALS AND METHODS

Antibodies and Reagents—The antiserum 29 was directed against a peptide of human ECE-1 catalytic domain (40). The antisera 1206 specific for ECE-1a and 1208 specific for ECE-1b/c/d were directed against peptides of the human ECE-1 cytosolic domain (56). The monoclonal antibody ECE-6 directed against ECE-1 has already been described (41). The antibodies directed against the following markers were also used: TGN38, provided by Dr. S. L. Milgram (University of North Carolina at Chapel Hill); ACTH, provided by the NIDDK, National Institutes of Health; transferrin receptor, from Zymed Laboratories Inc.; Cation-independent mannose-6-phosphate receptor, provided by Dr. W. J. Brown (Cornell University); lamp-1, from the Developmental Study Hybridoma Bank (University of Iowa); cathepsin D, from Santa Cruz Biotechnology (Santa Cruz, CA); M2 monoclonal antibody directed against the FLAG epitope, from Upstate (Charlottesville, VA); the proprotein convertase furin, from Alexis (San Diego, CA). Alexa Fluor-546 transferrin and Lysotracker Green were from Molecular Probes (Eugene, OR). The rab7-GFP construct was kindly provided by Dr. C. Bucci (Università di Napoli 'Federico II', Italy), and the dynamin-2-GFP wild type and K44A mutant by Dr. M. McNiven (Mayo Clinic, Rochester). Furin cDNA was a gift from Dr. J. W. Creemers (University of Leuven, Belgium). Bafilomycin A1 was from Kamiya (Seattle, WA). *Clasto*-lactacystin was from Calbiochem (San Diego, CA).

Cell Culture—AtT-20 cells were maintained at 37 °C in 5% CO_2, in high glucose Dulbecco's modified Eagle's medium (DMEM) (Invitrogen Life Technologies) containing 10% NuSerum IV (Becton Dickinson, Franklin Lakes, NJ), and 2.5% fetal bovine serum (Invitrogen Life Technologies). AtT-20 cells were provided by Dr. R. E. Mains (Johns Hopkins University School of Medicine). Transfected cell lines were cultivated with either one or both of the following selection agents: 200 μg/ml G418 (Invitrogen, Carlsbad, CA); 50 μg/ml zeocin (Invitrogen Life Technologies). The human microvascular dermal endothelial cell line HMEC-1 was cultivated in MCDB-31 containing 20% fetal bovine serum, 10 ng/ml epidermal growth factor, and 1 μg/ml hydrocortisone (42).

Site-directed Mutagenesis and Transfection—Mutations were generated by PCR-mediated methods. The PCR fragments were cloned into pCDNA3.1 (Invitrogen Life Technologies) containing the human ECE-1 cDNA (39), at the *Nhe*I and *Hin*dIII restriction sites. All the cDNA fragments generated by PCR were verified by DNA sequencing after insertion in pCDNA3.1. The sequence coding for the FLAG epitope was added at the 3′-end of ECE-1 cDNA by PCR. AtT-20 cells were transfected using LipofectAMINE 2000 according to the manufacturer's recommendations (Invitrogen Life Technologies). Clones were first screened by immunoblotting, and then by immunofluorescence in order to select cells with a homogenous expression. 2–4 independent clones were analyzed for each construct.

For the double transfected cell lines, AtT-20 cells were first transfected with pCDNA3.1 coding for ECE-1b with a C-terminal FLAG epitope and for the G418 resistance. A stable clone was then transfected with pcDNA3.1 coding for ECE-1a and for the zeocin resistance.

For transient expression of rab7-GFP and dynamin-2-GFP, cells were transfected on coverslips using LipofectAMINE 2000 for 3 h and treated for immunofluorescence 16–20 h later.

Immunofluorescence—Cells were seeded on 14-mm coverslips, cultivated for 40–48 h, and fixed with cold methanol for 5 min. They were then washed with PBS, and nonspecific binding was saturated with either 1% BSA or 10% normal goat serum in PBS. They were then incubated with the primary antibodies in 0.1% BSA or 1% normal goat serum in PBS. Goat or donkey antibodies directed against rabbit IgG were coupled to Alexa Fluor-488 or Alexa Fluor-555 (Molecular Probes) or to Cy5 (Amersham Biosciences). Goat antibodies directed against mouse IgG and donkey antibodies directed against goat IgG were coupled to tetramethylrhodamine (TRITC) (Jackson Immunoresearch) or Alexa Fluor-546 (Molecular Probes). For antibody uptake experiments, cells were preincubated for 30 min in DMEM containing 0.1% BSA. They were then incubated with the 29 antiserum in the presence of 0.1% BSA and 5 mM dithiothreitol for 30 min at 37 °C as previously described (39). Cells were then fixed with methanol and incubated with a secondary antibody coupled to Alexa Fluor-488. In some experiments, cells were preincubated in DMEM containing 0.1% BSA and incubated for 20 min at 37 °C with 25 μg/ml Alexa Fluor-546 transferrin before fixation.

Coverslips were mounted with Mowiol and observed with a Leica TCS SP2 confocal microscope equipped with three external lasers (488, 543, and 633 nm) (Leica Microsystems). Images were acquired with a ×63/1.32 PL APO objective lens. All the double labeling experiments were analyzed in sequential scanning mode. The confocal sections always corresponded to the medium level of the cells, except for the ACTH-labeled cells. In these cells, sections corresponded to the basal level of the cells in order to detect the secretory granules. The perinuclear zone thus appeared more diffuse in these images. All the images correspond to 80 × 80 μm fields.

Pre-embedding Immunoperoxidase Staining—Labeling was performed directly on AtT-20 cells as previously described (43). Cells were plated in 35-mm tissue culture dishes. They were fixed in periodate-lysine-paraformaldehyde for 2 h at room temperature, washed, preincubated in 50 mM NH4Cl, and permeabilized with 0.005% saponin. After incubation with specific rabbit antibodies, cells were incubated with goat Fab anti-rabbit IgG conjugated with peroxidase (Biosys; Compiègne, France). After washing, cells were postfixed in 1% glutaraldehyde, and the peroxidase activity was visualized using 3,3′-diaminobenzidine tetrahydrochloride. Cells were postfixed in 1% osmium tetroxide, dehydrated, and embedded *in situ* in Epon. Selected areas of immunoreactive cells were sectioned as previously described. Ultrathin sections were examined at the electron microscope without further staining.

Metabolic Labeling and Immunoprecipitation—150,000 cells were seeded in 12-well plates. 40 h later, cells were labeled for 30 min with 100 μCi/ml of [^{35}S]methionine and cysteine (ProMix, Amersham Biosciences, Piscataway, NJ). They were then directly extracted or chased in DMEM containing 2% fetal bovine serum. Cells were extracted on ice with 0.5% Nonidet P-40 and 0.5% deoxycholate in 25 mM Tris-HCl pH 7,4 containing 100 mM NaCl and 5 mM EDTA. Before extraction, a protease inhibitor mixture (Sigma) was added to the lysis buffer. Lysates were spun for 10 min at 15,000 × *g* at 4 °C. The supernatant was collected and ECE-1 was immunoprecipitated, using either the 29 or 1206 or 1208 antibodies. All steps were done at 4 °C. Briefly, extracts were precleared in the presence of protein A coupled to Sepharose CL-4B (Amersham Biosciences). The supernatants were then incubated for 2 h in the presence of the antiserum, and the immune complexes were precipitated using protein A coupled to Sepharose CL-4B, washed once with the lysis buffer, once with PBS containing 0.5 M NaCl, and twice with PBS. Immunoprecipitated material was analyzed by SDS-PAGE. Gels were directly exposed to a Biomax film (Kodak). For the measurement of the degradation rate of ECE-1, quantitative analysis of radiolabeled material was done using an FX Molecular Imager and QuantityOne software (Bio-Rad, Hercules, CA). In order to study the degradation pathway of ECE-1b, cells were chased in the presence of 10 mM NH_4Cl or 1 μM Bafilomycin A1 or 1 μM *clasto*-lactacystin.

In some experiments, immunoprecipitated material was analyzed by immunoblotting. Proteins were separated by SDS-PAGE and transferred to polyvinylidene difluoride membranes. Nonspecific binding was

saturated in 10 mM Tris, 150 mM NaCl, pH 7.4 containing 5% low fat milk, and membranes were then incubated with the antibodies in the same buffer containing 0.5% low fat milk and 0.2% Tween-20. Alkaline phosphatase activity was detected using Attophos (Promega, Madison, WI) as a substrate and analyzed with an FX Molecular Imager and Quantity One software (Bio-Rad).

Determination of ECE-1 Activity—ECE-1 activity was measured using the BK2 peptide (aminomethylcoumarin-RPPGFSAFR-dinitrophenyl) as a substrate. The proteolysis of this quenched peptide at the Ala^7–Phe^8 bond by ECE-1 has already been characterized (44). The BK2 peptide was synthesized by Sigma-Genosys (The Woodlands, TX). 5000 cells were seeded per well of 96-well plates 40 h before activity measurement. Cells were preincubated 60 min in serum-free medium. They were then washed twice, and the assay was performed in Hank's Balanced Salt Solution containing 25 mM PIPES pH 6.5, in the presence of the following protease inhibitors: 1 mM AEBSF, 800 nM aprotinin, 20 μM leupeptin, 36 μM bestatin, 15 μM pepstatin A, and 14 μM E-64. The experiments were performed in the presence of 30 μM of the BK2 peptide. Cells were preincubated in the reaction buffer, in the presence or absence of 0.4% *n*-octyl-glucoside, at 37 °C for 15 min prior to addition of the substrate. The activity was assessed in triplicate wells for 30 min at 37 °C. Fluorescence was measured using a Gemini XS microtiter plate reader and pro-Max software (Molecular Device, Sunnyvale, CA) using 330 nm excitation and 395 nm emission wavelengths. The protein content was determined in a duplicate 96-well plate using the BCA protein assay (Pierce). ECE-1 activity was normalized to the expression level of the enzyme in each clone as measured by the activity detected in the presence of 0.4% of the detergent *n*-octyl-glucoside. Values are relative fluorescence units per min per μg of total proteins. They corresponded to the mean activity determined in triplicate culture wells. Experiments were reproduced two or three times and provided similar ratios of extracellular per total activity.

RESULTS

Characterization of ECE Isoforms in AtT-20 Cells—Mouse pituitary corticotrope AtT-20 cells were used to analyze the function of ECE-1 isoforms in neuroendocrine cells. The four ECE-1 isoforms were stably expressed in AtT-20 cells at similar levels. We first analyzed the maturation of ECE-1 by metabolic labeling (Fig. 1*B*). ECE-1 forms disulfide-bound dimers (20–22). Immunoprecipitation demonstrated that the 4 ECE-1 isoforms dimerized with similar kinetics as only the dimeric form was detected after a 2-h chase. At the end of the labeling period, a monomeric form could be detected together with a diffuse band of higher molecular weight. This band disappeared after the chase period, which suggested that it corresponded to intermediate dimers of ECE-1 either incompletely folded or incompletely glycosylated. These experiments also provided information concerning the degradation rate of ECE-1. Whereas the half-life of ECE-1a, 1c, and 1d was ~7 h, ECE-1b was degraded much more rapidly, with a half-life of ~3 h.

We then investigated the subcellular distribution of ECE-1 isoforms in AtT-20 cells by immunofluorescence (Fig. 1*C*). No endogenous ECE-1 was detected in wild type cells. ECE-1a and 1c were mainly present at the plasma membrane, whereas ECE-1b was detected inside the cells. A similar pattern of localization was observed in transfected CHO cells (37, 39). In AtT-20 cells, ECE-1d was faintly detected on the plasma membrane and was mainly found inside the cells. We had observed the prominent labeling of the plasma membrane for this isoform in CHO cells (30). This difference could result from the higher level of expression in CHO cells as a strong labeling of the plasma membrane was also detected in AtT-20 cells expressing higher levels of ECE-1d. The major intracellular localization of ECE-1d was also observed when a GFP-ECE-1d chimera was expressed in AtT-20 cells and when ECE-1d was expressed in the epithelial MDCK cells (data not shown). In addition, the same subcellular distributions were observed using different antisera directed against the catalytic domain of ECE-1 (29 and ECE-6) or directed against the cytosolic domains of ECE-1 isoforms (1206 and 1208), as well as using ECE-1 isoforms tagged with a FLAG epitope. However, there were some differences in the distribution of the intracellular isoforms: ECE-1d labeled a unique diffuse area in the perinuclear region, whereas ECE-1b was concentrated in numerous large vesicles dispersed in the cytoplasm.

We further investigated the presence of ECE-1 on the plasma membrane by measuring its extracellular activity. For this purpose, cells were incubated in the presence of the fluorescent quenched peptide BK2. Some endogenous processing of BK2 was detected with wild type AtT-20 cells (Fig. 1*D*). It was inhibited by 100 μM ortho-phenantrolin and by 1 mM EDTA, but not by 100 μM phosphoramidon, the common NEP/ECE-1 inhibitor. The processing detected with cells expressing ECE-1a was ~3-fold higher both in the extracellular medium and in the presence of the detergent *n*-octyl-glucoside. It was not inhibited by 6 μM batimastat, a matrix metalloprotease inhibitor, nor by 100 μM thiorphan, an inhibitor of NEP, nor by 1 μM lysinopril, an inhibitor of angiotensine converting enzyme. On the other hand, 1 μM phosphoramidon almost completely inhibited BK2 processing by AtT-20 cells expressing ECE-1 (data not shown). Background activity detected with wild type AtT-20 cells was subtracted from the activity measured with AtT-20/ECE-1 cells. ECE-1a and 1c displayed a high extracellular activity, whereas ECE-1d and ECE-1b extracellular activity was much lower, in agreement with the immunofluorescence data (Fig. 1*E*).

Taken together, these experiments provide new data on the most recently identified isoform, ECE-1d. In AtT-20 cells, this isoform was mainly present in intracellular compartments although low levels could also be detected at the plasma membrane. In addition, these experiments demonstrate that ECE-1a, 1b and 1c displayed the same localization in neuroendocrine cells, as in fibroblasts (37, 39).

ECE-1b and 1d Were Not Concentrated in the Secretory Pathway—The labeling observed with ECE-1b and ECE-1d suggested that these isoforms could be targeted to different intracellular compartments (Fig. 1*C*). Previous studies had proposed that ECE-1b specifically functioned in the intracellular production of endothelin. Such a hypothesis would require the concentration of ECE-1b in the secretory pathway. Thus, we investigated the expression of ECE-1b and 1d in the secretory pathway by double immunofluorescence. Big endothelin is first generated in the trans-Golgi network (TGN) by the processing of pro-endothelin by furin or PC7/PC8/LPC (11, 12), both resident enzymes of this compartment (Refs. 45 and 46 and see Fig. 5*C*). We thus investigated the presence of ECE-1b and −1d in the TGN, using TGN38 as a marker. These isoforms were not concentrated in this compartment (Fig. 2*A*). We also investigated the presence of ECE-1b and 1d in the regulated secretory pathway using ACTH as a marker. Proopiomelanocortin, the precursor of ACTH, is the secretory product specific for AtT-20 cells. The antibody directed against ACTH labeled the juxtanuclear zone, corresponding to the Golgi apparatus, and the secretory granules accumulated in the cell processes (*arrowhead* in Fig. 2*B*). ECE-1b and 1d colocalization with ACTH was faint in the Golgi zone, and absent in the secretory granules (Fig. 2*B*). We could further demonstrate that these ECE-1 isoforms were not concentrated in the secretory pathway, as they were not redistributed to the endoplasmic reticulum by brefeldin A as ACTH was (data not shown).

These experiments demonstrated that ECE-1b and 1d were present in the Golgi zone to a limited extent. Unlike the proprotein convertase furin, which cleaves pro-endothelin in the

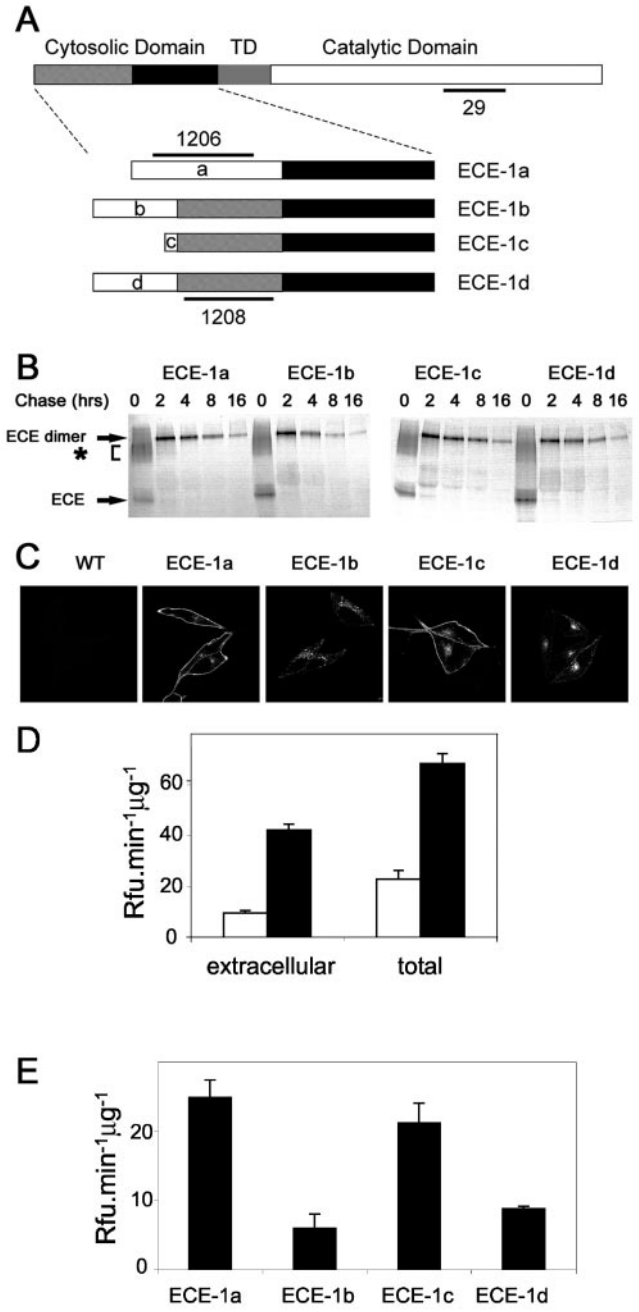

FIG. 1. **Expression of ECE-1 isoforms in AtT-20 cells.** *A*, schematic representation of the structure of ECE-1 isoforms. The peptides used for generating the polyclonal antibodies 29, 1206, and 1208 are indicated by the bars. *B*, biosynthesis of ECE-1 isoforms. AtT-20 cells expressing ECE-1a, ECE-1b, ECE-1c, ECE-1d were metabolically labeled for 30 min and chased for the indicated time periods. ECE-1 was immunoprecipitated with antiserum 29. Immunoprecipitates were separated by SDS-PAGE under nonreducing conditions and radiolabeled proteins were detected by autoradiography. Monomeric and dimeric ECE-1 are indicated by *arrows*. The *asterisk* corresponds to intermediates in the formation of dimers. *C*, subcellular localization of ECE-1 isoforms. AtT-20 cells (*WT*) and stable clones expressing ECE-1a, ECE-1b, ECE-1c, and ECE-1d were fixed with cold methanol and ECE-1 immunoreactivity was detected using the monoclonal antibody ECE-6. *D* and *E*, catalytic activity of the ECE-1 isoforms. *D*, cells were incubated in the presence of BK2 as described under "Materials and Methods." Wild type (*open bars*) and ECE-1a-expressing cells (*closed bars*) were incubated in the absence or presence of *n*-octyl-glucoside in order to measure the extracellular and the total activity, respectively. *E*, catalytic activity was measured from cells expressing each ECE-1 isoform. Activity of wild type AtT-20 cells was subtracted and extracellular activity was normalized to ECE-1 expression as measured by total ECE-1 activity in the presence of *n*-octyl-glucoside. Results are expressed as relative fluorescence unit per μg of total protein per min.

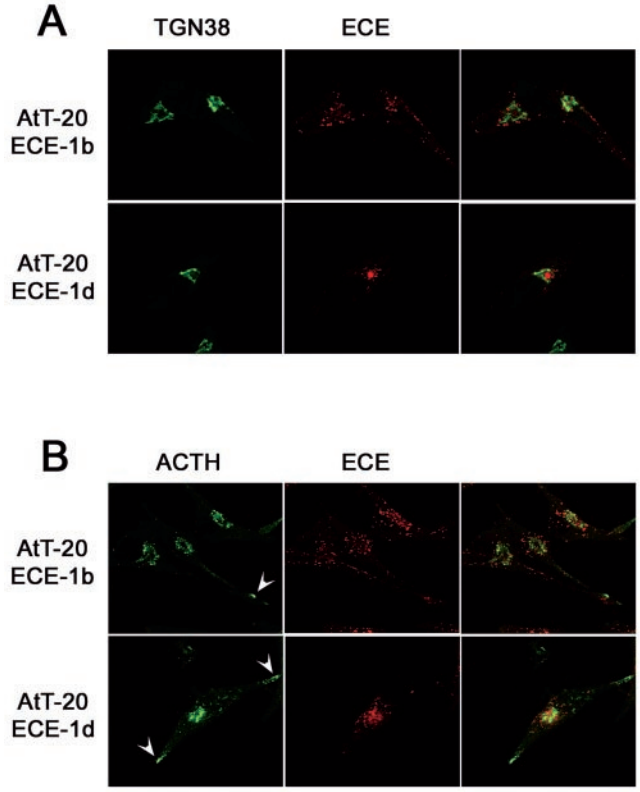

FIG. 2. **ECE-1b and 1d are not concentrated in the secretory pathway.** AtT-20 cells stably expressing either ECE-1b or ECE-1d were fixed with cold methanol. ECE-1 co-immunolocalization was performed using polyclonal antibodies directed against TGN38 (*A*), a marker for the TGN, or ACTH (*B*), a marker for the regulated secretory pathway, and the monoclonal antibody ECE-6. ACTH was present in the Golgi zone and in the secretory granules accumulated in the cell processes (*arrowheads*).

TGN, ECE-1b, and 1d were accumulated in a compartment that is distinct from the secretory pathway.

ECE-1b and 1d Were Concentrated in Distinct Endosomal Compartments—The strong intracellular staining of ECE-1b and 1d that was not localized to the secretory pathway suggested that these isoforms could be concentrated in the endosomal system. We thus investigated their localization using the transferrin receptor and internalized transferrin as markers for recycling endosomes, mannose-6-phosphate receptor and rab7 as markers for late endosomes/multivesicular bodies, and cathepsin D and Lamp-1 as markers for lysosomes. ECE-1d was completely co-localized with the transferrin receptor, which was detected in the diffuse perinuclear compartment described above (Fig. 3*A*). Similar results were obtained using internalized transferrin as a marker (data not shown). These data demonstrated that ECE-1d was concentrated in the recycling endosomes. ECE-1b was also detected in the recycling endosomes. However, the large vesicles that contained most of the ECE-1b labeling were not labeled with the transferrin receptor. On the other hand, ECE-1b was partially co-localized with a rab7-GFP chimera, whereas ECE-1d was not (Fig. 3*B*). As already demonstrated for other endosomal proteins (47), the overexpression of rab7-GFP did not modify the distribution of ECE-1b and 1d. In agreement with these results, ECE-1b was also partially co-localized with the mannose-6-phosphate receptor, a late endosome marker (data not shown). ECE-1b and 1d were not detected in lysosomes, as demonstrated by cathepsin D (Fig. 3*C*) or Lamp-1 (data not shown) labeling or with the lysosomal marker Lysotracker (data not shown). The same pattern of co-localizations with endosome markers was ob-

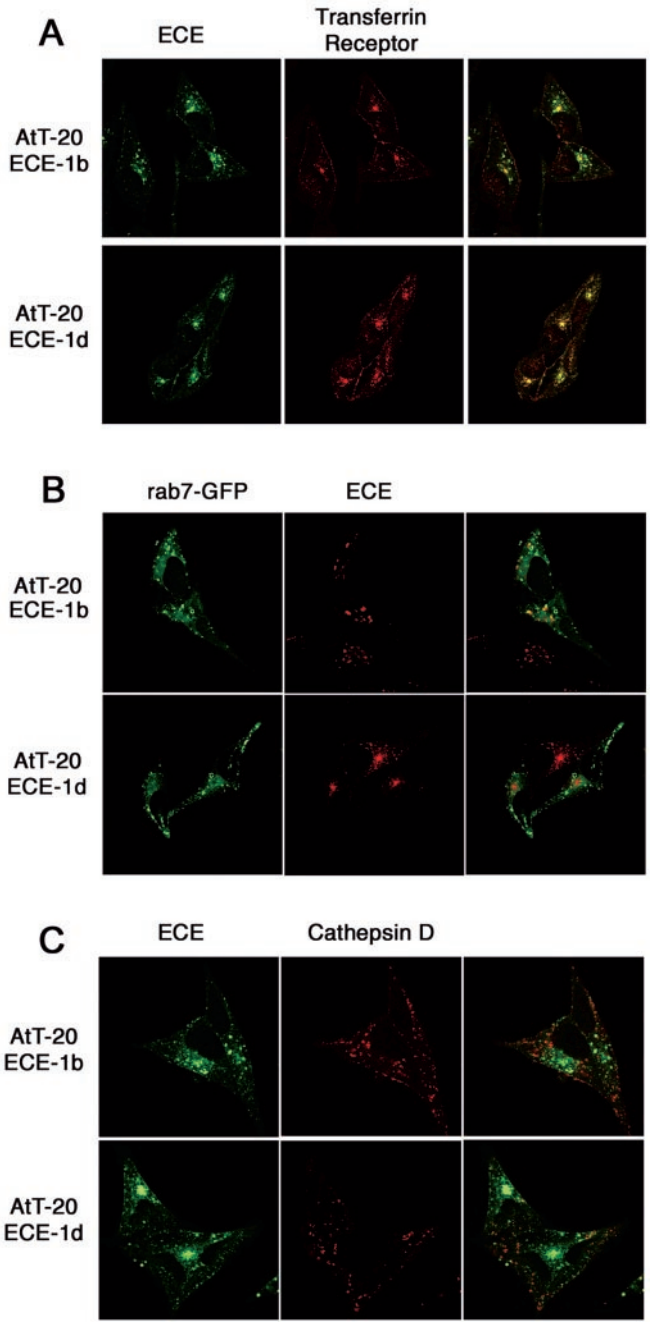

FIG. 3. **ECE-1b and 1d are concentrated in endosomal compartments.** AtT-20 cells expressing either ECE-1b or ECE-1d were fixed with cold methanol. ECE-1 immunoreactivity was detected using antiserum 29 (*A*, *B*, and *C*). The transferrin receptor, a marker for the recycling endosomes, was immunolocalized with a monoclonal antibody (*A*) and cathepsin D, a marker for lysosomes, with a goat antibody (*C*). Alternatively, AtT-20 cells stably expressing either ECE-1b or ECE-1d were transiently transfected with a rab7-GFP chimera (*B*), a marker for the late endosomes/multivesicular bodies, and ECE-1 immunoreactivity was detected 16 h after transfection.

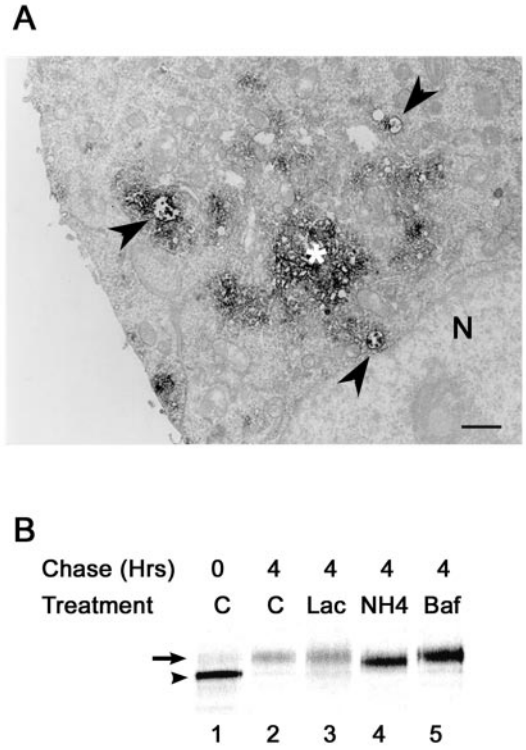

FIG. 4. **ECE-1b is present in multivesicular bodies.** *A*, ECE-1b was detected by immunoelectron microscopy using the 29 antiserum. Immunoperoxidase activity was present both in aggregated small vesicles that corresponded to the recycling endosomes (*asterisk*) and in the large multivesicular bodies that surrounds them (*arrowheads*). *Bar*, 1 μm. *B*, degradation of ECE-1b. AtT-20 cells expressing ECE-1b were metabolically labeled for 30 min and directly extracted (*lane 1*) or chased for 4 h under control conditions (*lane 2*) or in the presence of 1 μM *clasto*-lactacystin (*lane 3*) or 10 mM NH4Cl (*lane 4*) or 1 μM Bafilomycin A1 (*lane 5*). ECE-1 was immunoprecipitated with antiserum 29. Immunoprecipitates were separated by SDS-PAGE under reducing conditions and radiolabeled proteins were detected with a Molecular Imager. *Arrowhead* indicates the position of core-glycosylated ECE-1. *Arrow* indicates the position of mature ECE-1.

served when ECE-1b and 1d were transiently expressed in HeLa cells (data not shown).

In order to further identify the large vesicles labeled with ECE-1b, we used electron microscope immunocytochemistry. These experiments demonstrated the presence of ECE-1b in multivesicular bodies, as identified by their morphology (Fig. 4*A*, *arrowheads*). We had already described the expression of ECE-1b in these structures in transfected CHO cells (39). In addition, ECE-1b was detected in a central zone consisting of aggregated small vesicles (Fig. 4*A*, *asterisk*). These membrane structures likely corresponded to the recycling endosomes that were co-labeled with the transferrin receptor and ECE-1b (Fig. 3*A*). Degradation of proteins is initiated in multivesicular bodies, the transport intermediate to lysosomes. The presence of ECE-1b in these organelles was thus in agreement with the rapid degradation of this isoform (Fig. 1*B*). We further investigated the degradation of ECE-1b with inhibitors (Fig. 4*B*). After a 4-h chase period, ECE-1 was completely glycosylated and most of the neosynthesized ECE-1 was degraded (Fig. 4*B, lane 2*). The lysosomotropic agent (NH_4Cl) and the vacuolar ATPase inhibitor Bafilomycin A1, which both prevent the luminal acidification of the pH, could block ECE-1b degradation. On the other hand, the cell-permeant proteasome inhibitor *clasto*-lactacystin had no effect on ECE-1b degradation.

ECE-1b and 1d Were Transiently Expressed at the Cell Surface—The detection of extracellular enzymatic activity from cells transfected with ECE-1b and ECE-1d suggested a higher level of expression on the plasma membrane than revealed by immunofluorescence. The transient presence of ECE-1b and ECE-1d at the cell surface could account for this difference. In order to investigate such possibility, we performed antibody uptake experiments. We used cells expressing ECE-1c as a control since this isoform was detected both at the cell surface and inside the cells (Fig. 1*C*). The cells were first incubated in the presence of the 29 antiserum, directed against the ectodomain, at 37 °C in order to detect internalized ECE-1. They were then fixed with methanol and the total ECE-1 content was

detected with the monoclonal ECE-6 antibody. AtT-20 cells expressing ECE-1c could uptake the 29 antiserum. The labeling of internalized ECE-1c completely overlapped that of total ECE-1c. In addition, both labeling provided a signal as intense, as shown by the yellow appearance on the merged image. These results suggested a high rate of recycling for this isoform. ECE-1b and ECE- 1d could also internalize the 29 antiserum (Fig. 5*A*), but the level of antibody uptake was much lower than for cells expressing ECE-1c. Antibody uptake was very faint in some cells expressing ECE-1b (*asterisk* in Fig. 5*A*). To confirm these results, AtT-20 cells expressing ECE-1b or ECE-1d were transiently transfected with either the wild type dynamin-2 or the dominant-negative K44A mutant. Dynamin-2 is involved in the internalization of plasma membrane proteins (for review see Ref. 48). Transfection of the wild type dynamin did not modify the distribution of ECE-1b and 1d. The K44A mutant prevents the endocytosis of plasma membrane proteins. When expressed with the dominant-negative mutant, ECE-1b and ECE-1d were detected at the cell surface (Fig. 5*B*). As a control, we investigated the effect of the expression of the dynamin mutant on the distribution of furin, the enzyme responsible for the first step in the processing of pro-endothelin. Furin was completely co-localized with TGN38 (Fig. 5*C*), as already described (45). The K44A dynamin mutant did not modify the distribution of furin nor of TGN38 (Fig. 5*C*). These data were in agreement with the concentration of ECE-1b and 1d in a compartment distinct from the TGN. They further demonstrated that these ECE isoforms were concentrated in some endosomal compartment cycling with the plasma membrane. Taken together, these data were in agreement with the extracellular activity from AtT-20 cells expressing ECE-1b and ECE-1d (Fig. 1*D*). They suggested that these isoforms were targeted to the endosomal system, both directly from the TGN and after transport to the plasma membrane. Recycling of ECE-1b and 1d was however occurring at a much lower rate than for the plasma membrane isoform ECE-1c.

Identification of the Signals Responsible for Targeting to the Endosomal Pathway—We have already shown that the intracellular localization of ECE-1b is due to two leucine-based motifs: one common to ECE-1b, 1c and 1d (Leu^{31}-Val^{32} in ECE-1b), and one specific for ECE-1b (Leu^{12}-Leu^{13}) (39). Interestingly, ECE-1d also contains a specific leucine-based motif (Val^{8}-Leu^{9}). In order to investigate the relative role of these motifs in targeting to different endosomes, we mutated these into alanines and exchanged them between ECE-1b and ECE-1d. The mutation of ECE-1b Leu^{31}-Val^{32} into Ala-Ala (b LV/AA) did not affect its sorting to the degradation pathway (Table I). On the other hand, the loss of the ECE-1b Leu^{12}-Leu^{13} (b LL/AA) motif reduced the degradation rate of ECE-1b (Table I). In agreement with these results, the distribution of the b LV/AA mutant was not modified (Fig. 6*C*), whereas the loss of the ECE-1b-specific LL motif (b LL/AA) resulted in an intracellular distribution resembling that of ECE-1d with increased presence of the enzyme at the cell surface (Fig. 6*A*). Thus, only the b-specific di-leucine motif is involved in the targeting to the degradation pathway. However, the nature of the residues in the di-leucine motif could not alone account for the rapid degradation of ECE-1b. First, the ECE-1b LL/VL mutant was degraded as rapidly as wild type ECE-1b (Table I) and displayed the same distribution as wild type ECE-1b (Fig. 6*B*). Second, the ECE-1d VL/LL mutant (d VL/LL) was not degraded as rapidly as ECE-1b (Table I). The distribution of this mutant however was slightly modified, and ECE-1d VL/LL was detected both in the central recycling endosomes and in surrounding large vesicles (Fig. 6*E*). In addition, the VL motif in ECE-1d was involved in the intracellular localization of this isoform, as its mutation into Ala-Ala could increase its plasma membrane targeting (Fig. 6*D*).

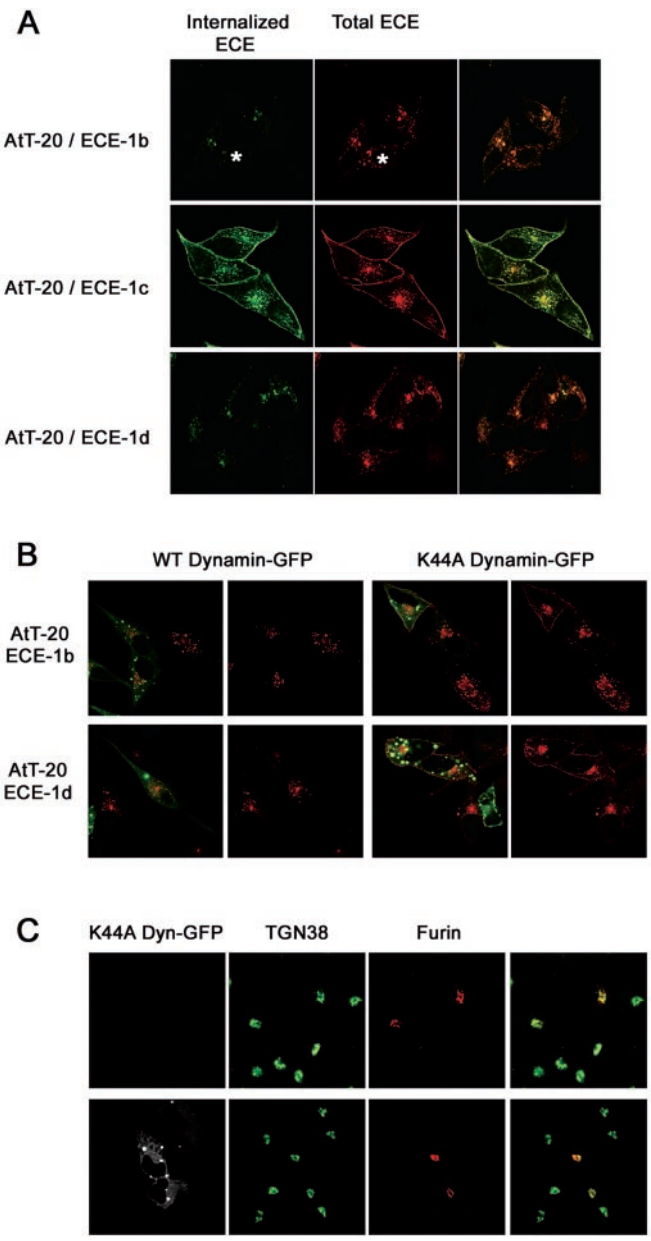

FIG. 5. **ECE-1b and ECE-1d are transiently expressed at the cell surface.** *A*, AtT-20 cells expressing ECE-1b, ECE-1c, or ECE-1d were incubated with antiserum 29 at 37 °C in order to detect the plasma membrane and internalized ECE-1. Cells were then fixed with cold methanol and incubated with the monoclonal antibody ECE-6 in order to detect the total ECE-1. Confocal analysis was performed using the same settings for internalized ECE-1 and for total ECE-1 in the three cell lines in order to provide semiquantitative information. A cell expressing ECE-1b unable to uptake antibody is shown (*asterisk*). *B*, AtT-20 cells expressing ECE-1b or ECE-1d were transiently transfected with the GFP chimera of either the wild type or the K44A mutant of dynamin-2 (*green*). ECE-1 immunoreactivity was detected with the 29 antiserum (*red*). Double transfected cells are identified on the overlay image, and the effect of the transfected protein on the distribution of ECE-1 is shown on the right image. *C*, wild type AtT-20 cells were transiently transfected either with furin alone or co-transfected with furin and the GFP chimera of the K44A mutant of dynamin-2. TGN38, a marker for the TGN, was detected with a polyclonal antibody and furin with the MON-139 monoclonal antibody. The *left panel* shows the GFP fluorescence in *black and white*. The merged image shows the co-localization of furin and TGN38 only.

Taken together, these results suggested that ECE-1b contained additional information responsible for its rapid degra-

TABLE I

The half life of wild type and mutant ECE-1b and 1d was calculated after performing pulse chase experiments as described under "Materials and Methods." Experiments were reproduced three times on 2–4 clones per mutation.

Construct name	Sequence	Half-life
		h
b	mrgvwpppvsallsalgmstykratldeedlvdsl	3
b LL/AA	mrgvwpppvsa**AA**salgmstykratldeedlvdsl	5, 5
b LL/VL	mrgvwpppvsa**VL**salgmstykratldeedlvdsl	4
b LV/AA	mrgvwpppvsallsalgmstykratldeed**AA**dsl	3, 5
b-d	mrgvwpppvsvlhlalqmsty	4
d	mealresvlhlalqmsty	7
d VL/AA	mealres**AA**hlalqmsty	7
d VL/LL	mealres**LL**hlalqmsty	5, 5

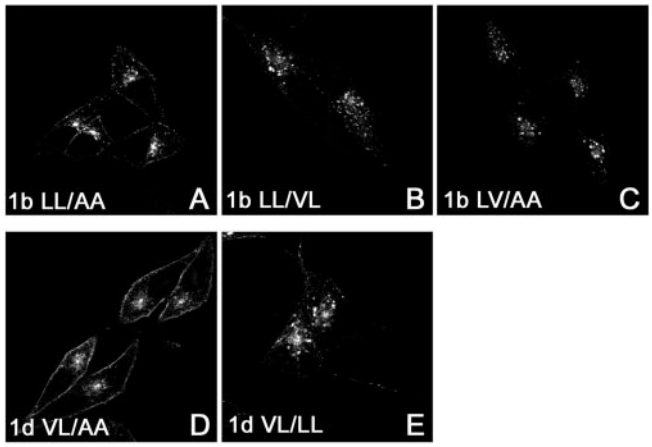

FIG. 6. **Leucine-based motifs are involved in the intracellular retention of ECE-1b and ECE-1d.** ECE-1 immunoreactivity was detected with the 29 antiserum in AtT-20 cells expressing the following mutants: *A*, 1b LL/AA; *B*, 1b LL/VL; *C*, 1b LV/AA; *D*, 1d VL/AA; *E*, 1d VL/LL.

dation. In order to test this hypothesis, we constructed a chimera consisting of the 10 N-terminal residues of ECE-1b followed by the Val^{8}-Leu^{9} motif of ECE-1d (b-d). This chimera was degraded as rapidly as ECE-1b, suggesting that another determinant important for ECE-1b degradation was present at the N terminus of the di-leucine motif (Table I). In order to identify a second signal involved, we mutated each residue between Gly^{3} and Ser^{10} into Ala (data not shown). This alanine scan could not identify another signal responsible for the rapid degradation of ECE-1b. These experiments suggested that, in addition to the di-leucine motif, the 10 N-terminal residues of ECE-1b contain some sorting determinants involved in the rapid degradation of this isoform but not encoded by the primary sequence.

Heterodimerization of ECE Isoforms—ECE-1 forms dimers bound by a disulfide bond at Cys^{412} in the extracellular domain (22). Our metabolic labeling experiments demonstrated that 100% of ECE-1 is expressed as dimers within 2 h after synthesis (Fig. 1*B*). We investigated the possibility that ECE-1 forms heterodimers in cells that express several isoforms. We used antiserum 1206 directed against the cytosolic domain of ECE-1a, and antiserum 1208 directed against a peptide common to the cytosolic domains of ECE-1b, 1c, and 1d. The specificity of these antibodies was demonstrated by immunofluorescence and immunoprecipitation of extracts from AtT-20 cells overexpressing ECE-1a or ECE-1b (Fig. 7, *A* and *B*). We investigated ECE-1 heterodimerization in endothelial cells that co-express endogenous ECE-1 isoforms. For this purpose, we used endothelial cells from the HMEC-1 cell line. These dermal microvascular cells express many endothelial markers (42). After metabolic labeling, the cell extracts were immunoprecipitated with the three antisera. We could detect ECE-1 isoforms in HMEC-1 cell extracts (Fig. 7*C*, *lanes 1–3*). Antiserum 1206 could detect very little ECE-1a. In order to analyze the presence of heterodimers, the 1206 immune complexes were denatured, and ECE-1b/c/d was immunoprecipitated with antiserum 1208 (Fig. 7*C*, *lane 4*). These experiments allowed the detection of ECE-1 dimers that contained ECE-1a, from the first immunoprecipitation, and either ECE-1b or 1c or 1d, as demonstrated by the second immunoprecipitation. The low efficacy of the 1206 antiserum in immunoprecipitation experiments, as compared with that of antiserum 29 directed against the catalytic domain of ECE-1 (Fig. 7*B*) prevented the quantitation of heterodimerization.

AtT-20 cell lines that co-expressed ECE-1a and 1b were generated to further investigate heterodimerization of ECE-1 isoforms (Fig. 8, *total lysate*). The presence of heterodimers was first investigated. ECE-1b was immunoprecipitated from the lysates with the 1208 antiserum and the immune complexes were analyzed by immunoblotting with either the 1206 or the 1208 antisera. These experiments demonstrated the presence of heterodimers containing ECE-1a and ECE-1b in the double transfected cells (Fig. 8, 1208 immunoprecipitate).

We then investigated whether ECE-1 heterodimerization affected the subcellular distribution of these isoforms. For this purpose, we used an ECE-1b construct that contained a FLAG epitope at the C terminus, in order to allow for the double immunolabeling using a monoclonal antibody directed against FLAG and antiserum 1206. The introduction of the FLAG epitope did not modify the intracellular distribution of ECE-1b (compare Figs. 1*C* and 9*A*). Upon co-expression of ECE-1bFLAG with ECE-1a, the localization of ECE-1a was partly shifted from the plasma membrane to intracellular vesicles. These vesicles also contained ECE-1b and displayed the pattern characteristic for this isoform (Fig. 9*A*). It is important to notice that, whereas the distribution of ECE-1a was modified, that of ECE-1b was not: no ECE-1b was detected at the plasma membrane upon co-expression with ECE-1a, even though some ECE-1a was still targeted to the plasma membrane.

To identify the intracellular compartment that contained both ECE-1a and ECE-1b, cells expressing either ECE-1a alone or together with ECE-1b were transiently transfected with the rab7-GFP chimera. Double immunofluorescence in these cells demonstrated that ECE-1a/ECE-1b dimers were partly present in late endosomes/vesicular bodies, as both isoforms were detected in some rab7 containing vesicles (Fig. 9*B*, *arrowheads* and *white* in merged *inset*). Some intracellular ECE-1a was not co-localized with rab7-GFP, even though it was co-localized with ECE-1b (Fig. 9*B*, *arrows* and *pink* in merged *inset*). This corresponded to the observation that ECE-1b alone was only partially present in late endosomes/multivesicular bodies (Figs. 3*B* and 4*A*). Control experiments demonstrated that ECE-1a was not present in rab7-containing vesicles when expressed alone (Fig. 9*B*).

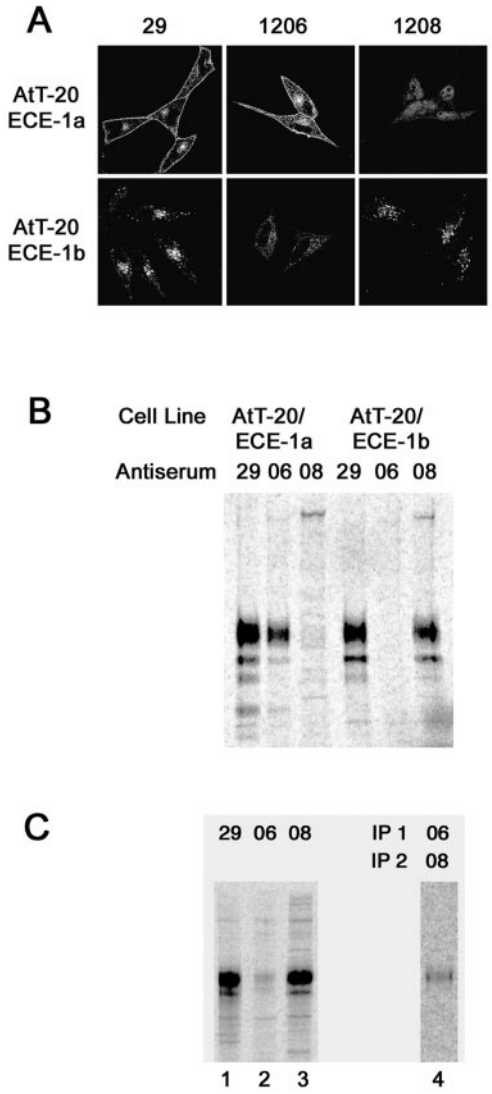

FIG. 7. **ECE-1 forms heterodimers in endothelial cells.** *A*, specificity of the antibodies directed against the cytosolic domain of ECE-1 isoforms. AtT-20 cells expressing ECE-1a or ECE-1b were fixed with methanol and labeled with either antiserum 29, directed against the ectodomain common to all isoforms, or antiserum 1206, directed against ECE-1a, or antiserum 1208, directed against ECE-1b/c/d. *B*, AtT-20 cells expressing ECE-1a or ECE-1b were metabolically labeled for 30 min and chased for 2 h. ECE-1 was immunoprecipitated with either the 29 or the 1206 or the 1208 antisera. Immunoprecipitates were separated by SDS-PAGE under reducing conditions. *C*, HMEC-1 cells were metabolically labeled for 1 h and chased for 2 h. ECE-1 was immunoprecipitated with either the 29 (*lane 1*) or the 1206 (*lane 2*) or the 1208 (*lane 3*) antiserum. Immunoprecipitates were separated by SDS-PAGE under reducing conditions. Alternatively, the 1208 immune complexes (IP1) were denatured and immunoprecipitated again using the 1206 antiserum (IP2). The IP2 immunoprecipitate was then separated by SDS-PAGE under reducing conditions (*lane 4*). Radiolabeled proteins were detected using a Molecular Imager. The material present in *lane 4* was detected using a higher sensitivity setting of the Molecular Imager.

To investigate the function of ECE-1 heterodimerization, we compared the extracellular activity of ECE-1a when expressed alone or in combination with ECE-1b. The insertion of the FLAG epitope at the C terminus of ECE-1b resulted in the loss of enzyme activity of this construct (Fig. 9*C*). Similar data were obtained by measuring ET-1 by ELISA after addition of big-ET-1 in the medium of cells expressing ECE-1bFLAG.[2] We

[2] R. Meidan and L. Muller, unpublished observations.

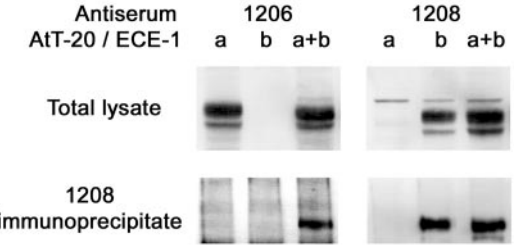

FIG. 8. **ECE-1 forms heterodimers in double transfected AtT-20 cells.** Cells expressing ECE-1a or ECE-1b/FLAG either alone or together were extracted. Total proteins were separated by SDS-PAGE under reducing conditions. Alternatively, ECE-1b was immunoprecipitated using the 1208 antiserum before reducing SDS-PAGE of the immune complexes. ECE-1 was detected using either the 1206 (*left panels*) or the 1208 antisera (*right panels*).

could not measure the effect of the FLAG epitope on the activity of ECE-1a/ECE-1bFLAG heterodimers. In such heterodimers, the FLAG epitope could either not alter or decrease the ECE-1a activity detected. Thus, our results could overestimate the ratio of extracellular per total ECE-1a activity in the double transfected cell lines. Upon co-expression of the two isoforms, the extracellular activity of ECE-1a per total activity was decreased (Fig. 9*D*). The activity was measured in three independent clones expressing ECE-1a alone and three independent clones expressing ECE-1a and ECE-1bFLAG. The mean value of the ratio of extracellular activity per total activity was 90.4, 59.7, and 80,6 for ECE-1a-expressing cells, and 60.5, 51.7, and 59.3 for double-transfected cells. Values are the mean of two or three independent experiments in which activity was determined in triplicate culture wells. The ratio of ECE-1a and ECE-1bFLAG in these clones was similar as estimated by Western blotting with the 1206 and 1208 antisera.

DISCUSSION

ECE-1 belongs to the family of NEP metalloproteases. Among these enzymes, ECE-1 has two unique characteristics: first, it is present and active both at the cell surface and in intracellular organelles; second, it exists as covalent dimers. In the present paper, we have investigated these two aspects of ECE-1 cell biology. Our experiments provided the first extensive analysis of the intracellular distribution of the 4 ECE-1 isoforms in the secretory pathway and in the endosomal system. The two isoforms localized in intracellular compartments, ECE-1b and 1d, displayed distinct but complementary patterns of distribution in the endosomal system: ECE-1d was present in the recycling endosomes and ECE-1b in the late endosomes/multivesicular bodies. Using biochemical methods, we could show that ECE-1 isoforms exist as heterodimers. The discovery of such heterodimers suggested a novel role for the isoform-specific targeting of ECE-1. We showed that the targeting signal responsible for the intracellular distribution of ECE-1b could redirect the plasma membrane ECE-1a to the endosomal system. These data demonstrated that the specific N terminus of ECE-1b constitutes a regulatory domain that is able to modify the distribution of other ECE-1 isoforms. Such a regulatory mechanism could be physiologically relevant as many cell types, including endothelial cells, co-express endogenously several ECE-1 isoforms (37, 30).

Our study was undertaken in the AtT-20 cell line due to the important function of endothelins in regulating the activity of neuroendocrine cells through autocrine and paracrine mechanisms (Ref. 49; for review see Ref. 3). Endothelins have been detected in the secretory granules of neuroendocrine cells (50), thus raising the possibility that ECE-1 was targeted to the secretory granules, like common neuroendocrine endopeptidases. Our results rejected the possibility that big-ET was

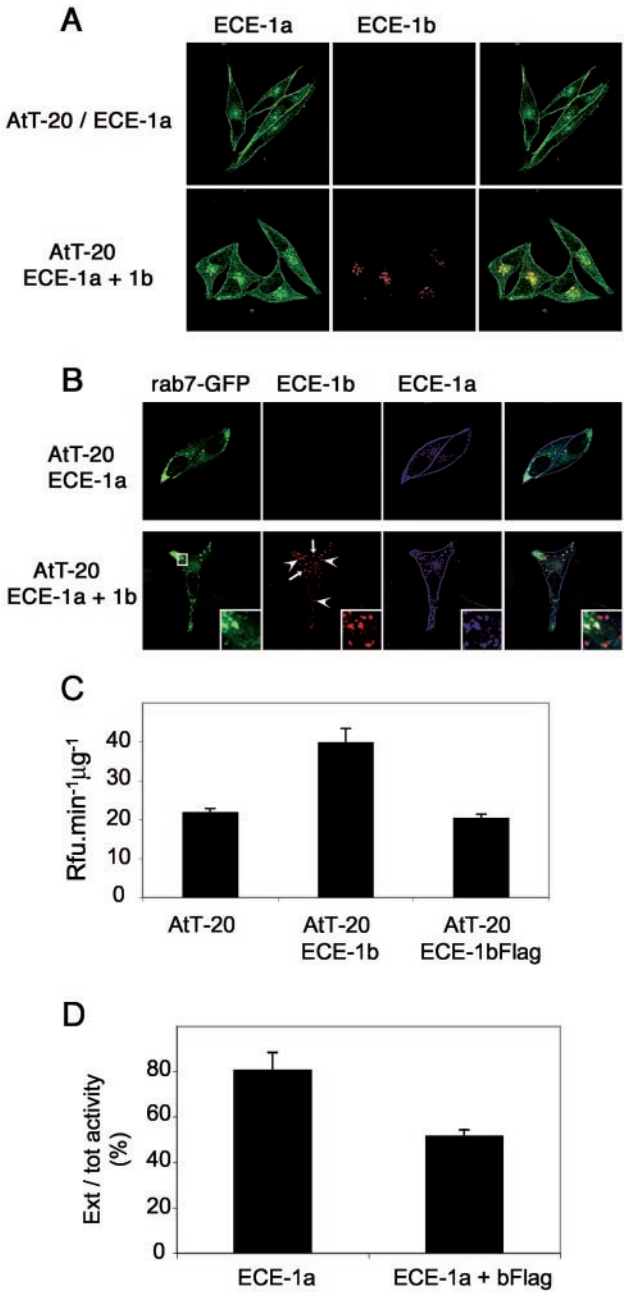

FIG. 9. **ECE-1b redistributes ECE-1a to intracellular vesicles.** *A*, AtT-20 cells expressing ECE-1a either alone or together with ECE-1bFLAG were fixed with methanol. ECE-1a was detected using the 1206 antiserum. ECE-1bFLAG was detected using the monoclonal M2 antibody. *B*, AtT-20 cells expressing ECE-1a either alone or together with ECE-1bFLAG were transiently transfected with a rab7-GFP chimera. ECE-1bFLAG was detected using the monoclonal M2 antibody and a secondary antibody coupled to Alexa Fluor-546. ECE-1a was detected using the 1206 antiserum and a secondary antibody coupled to Cy5. *Arrows* indicate double labeling of ECE-1a and ECE-1bFLAG. *Arrowheads* indicate triple labeling of vesicles. *C*, total activity from wild type AtT-20 cells or from cells expressing ECE-1b or ECE-1bFLAG was determined in the presence of 0.4% *n*-octyl-glucoside. Results are expressed as relative fluorescence unit per μg of total protein per min. *D*, catalytic activity was measured from cells expressing either ECE-1a alone or together with ECE-1bFLAG. Activity of wild type AtT-20 cells was subtracted, and the ratio of extracellular per total activity was calculated. Values are the mean of three independent experiments in which activity was measured in triplicate culture wells.

processed in secretory granules, as none of the intracellular isoforms were detected in the secretory granules. Our data thus suggested that the mature endothelin detected in the secretory granules might result from processing in the TGN. Processing of pro-endothelin by furin in this compartment is the first step that is required for ECE-1 to release endothelin from its precursor (51). Even though we did not find that ECE-1 was concentrated in the TGN, like furin is (45), ECE-1 is transported through this compartment during biosynthesis. The intracellular processing of big-ET in the TGN would thus not be a specialized function for any ECE-1 isoform. Indeed, we have already shown that ECE-1a, a plasma membrane isoform, could generate endothelin in the secretory pathway as well as in the extracellular medium (16). Whereas ECE-1b and ECE-1d could generate endothelin in the secretory pathway, these isoforms should not be considered more specific than ECE-1a or 1c for this processing. In support of this, big-ET is the main species secreted from cells that co-express pre-pro-endothelin and an intracellular isoform of ECE-1, thus indicating the low efficiency of intracellular processing of big-ET by ECE-1 (14). On the other hand, ECE-2 could specifically fulfill this role as it displays the acidic optimum pH required for efficient conversion of precursors in the lumen of the TGN and the secretory vesicles (24), and as 2 of the 4 recently identified isoforms of ECE-2 were found in intracellular compartments (33).

Previous studies aimed at identifying the intracellular compartments containing ECE-1b have produced controversial results. ECE-1b was detected in the Golgi apparatus, where it was co-localized with the Golgi marker wheat germ agglutinin in endothelial cells (35) and with TGN38 in transfected fibroblasts (37, 39). In addition, the presence of ECE-1b in late endosomes/multivesicular bodies has been described in transfected epithelial cells and fibroblasts (38, 39). Our results were in agreement with these latter studies. In addition, we demonstrated that ECE-1d was also present in the endosomal system, but concentrated in the recycling endosomes. We showed that ECE-1b and 1d were cycling between the plasma membrane and endosomes using three different lines of evidence: first, extracellular activity was detected from cells expressing ECE-1b and 1d; second, cells expressing these isoforms were able to capture antibodies directed against the ectodomain; third, expression of a dominant negative mutant of dynamin, which blocks internalization of proteins, retained these ECE-1 isoforms at the plasma membrane, but had no effect on furin and on TGN38. In agreement with these results, ECE-1b was co-localized with rab5, a marker for early endosomes, which is the first intracellular compartment where endocytic vesicles fuse (38).

The ECE-1b-specific di-leucine motif was responsible for the intracellular retention of this isoform (52, 39). In the present study, we demonstrated that the intracellular localization of ECE-1d also relies on the presence of a specific leucine-based motif (Val^{8}-Leu^{9}). We had shown that a second leucine-based motif (Leu^{31}-Val^{32}), common to ECE-1b, 1c and 1d, was also involved in ECE-1b intracellular retention (39). Here we found that this signal is not involved in ECE-1b degradation. On the other hand, the ECE-1b specific di-leucine motif (Leu^{12}-Leu^{13}) was responsible for the rapid degradation of this isoform. This motif alone was however not sufficient. Even though leucine-based motifs have been implicated at multiple steps of intracellular sorting in the TGN, the endosomes and the plasma membrane (for review see Ref. 53), the determinants responsible for the specificity of the transport steps involved remain to be identified (54). Several lines of evidence suggested that the sorting of ECE-1b relied on additional signal to the LL motif: first, the mutation of the ECE-1b LL motif only slightly increased the plasma membrane localization, compared with the mutation of ECE-1d VL motif; second, exchanging the VL and

LL motifs modified ECE-1d degradation and localization, but not that of ECE-1b; third, the chimera containing the N-terminal residues of ECE-1b upstream of the VL motif of ECE-1d resulted in the rapid degradation of this construct. Our results suggested that ECE-1b N terminus encodes another complementary signal that does not reside in the primary structure. The additional signal could correspond to a secondary structure or to a post-translational modification that would increase the affinity of the di-leucine motif for an associated protein responsible for sorting to the degradation pathway. In the case of bovine isoforms of ECE-1, Emoto *et al.* (55) have provided evidence for the targeting of bovine ECE-1b to the plasma membrane, and for the sorting of bovine ECE-1a to lysosomes (55). It should be noted that bovine ECE-1b corresponds to human ECE-1c, which we also found targeted to the plasma membrane, and that bovine ECE-1a is poorly conserved with human ECE-1a. Indeed, the targeting signals responsible for bovine ECE-1a sorting are not present in human ECE-1.

The detection of ECE-1 isoforms in the endosomal system could correspond to some novel physiological function of this enzyme, as big-ET is not present in these compartments. Endosomal ECE-1 could constitute an intracellular pool that could be rapidly translocated to the plasma membrane upon stimulation of the cells, as suggested by the cycling of ECE-1b and ECE-1d between endosomes and plasma membrane. Alternatively, the intracellular retention of some ECE isoform could regulate the distribution of other isoforms through direct protein interaction. ECE-1 is expressed as disulfide-linked dimers, but the role of ECE-1 dimerization has not yet been found (20–22). We have already showed that ECE-1 is present only as dimers on the plasma membrane of endothelial cells (56). The present analysis of ECE-1 biosynthesis demonstrated that the complete dimerization of ECE-1 is a feature common to the 4 isoforms. Dimerization occurs rapidly after synthesis, most probably in the endoplasmic reticulum as we could observe the transient appearance of dimer intermediates that most likely corresponded to incompletely glycosylated or unfolded ECE-1. The Cys^{412} residue, present in the catalytic domain, is responsible for the dimerization (22). The role of ECE-1 dimerization has been investigated using site-directed mutagenesis of this cysteine. Mutation into a serine did not modify the glycosylation and the subcellular distribution of ECE-1. However, this mutation slightly modified the enzymatic characteristics of ECE-1 (22, 57).

Here, we provided evidence for the formation of heterodimers in endothelial cells endogenously co-expressing several isoforms. The investigation of the formation of heterodimers in these cells was however limited due to the low level of expression of ECE-1a, and to the lack of antibodies specific for either ECE-1b or 1c or 1d. Therefore, we generated AtT-20 cell lines that co-expressed ECE-1a, the isoform with the higher plasma membrane expression, and ECE-1b, which displays the more stable intracellular localization. In double transfected cells we could confirm the presence of heterodimers. Both isoforms were colocalized in intracellular vesicles and the extracellular activity of ECE-1a was decreased. In addition, triple labeling experiments demonstrated that ECE-1a was translocated to the late endosomes/multivesicular bodies that contained ECE-1b. Importantly, heterodimerization of these isoforms did not increase the expression of ECE-1b at the plasma membrane, thus demonstrating the dominant role of ECE-1b sorting signals. This was in agreement with the active sorting of ECE-1b to endosomes through a di-leucine motif, whereas ECE-1a might be transported to, and maintained at, the plasma membrane by the lack of a sorting signal rather than by active sorting.

Taken together, these data suggested that heterodimerization could regulate ECE-1 extracellular activity through the translocation of the plasma membrane isoform to intracellular compartments. Such a mechanism could be physiologically relevant at two levels. First at the expression level: heterodimerization could be directly regulated by the expression of each isoform. In fact, our experiments suggested that ECE-1 dimerization occurred early in the secretory pathway. The expression of ECE-1 isoforms is controlled by the presence of alternate promoters in the gene structure (29, 30, 34). Recent studies have provided evidence for the isoform-specific regulation of expression (58–61). Heterodimerization could thus modulate the shift from plasma membrane activity to intracellular activity generated at the level of translation. In support of this hypothesis, the ECE-1 activity measured during liver wound healing was unchanged whereas the expression of ECE-1 isoforms was differentially regulated (58). An additionnal level of regulation could correspond to the exchange of the dimerized isoforms. Recent studies have provided evidence for the presence of protein disulfide isomerase activities at the plasma membrane (62–65). In this regard, the cycling of ECE-1b and ECE-1d between the plasma membrane and endosomes could provide a mean for internalizing the plasma membrane ECE-1a and ECE-1c through disulfide exchange mediated by a plasma membrane disulfide isomerase.

Processing enzymes are regulated through different pathways, like activation of proenzymes or regulation of activity by endogenous inhibitors. ECE-1 is not synthesized as a proenzyme, and no associated protein or endogenous inhibitor has been documented so far. In the present study, we propose that heterodimerization of ECE-1 isoforms could constitute a mean for regulating their distribution and, subsequently, their extracellular activity. Heterodimerization could also be important for other metalloproteases like aminopeptidases and matrix metalloproteases, which are known to form disulfide-linked dimers.

Acknowledgments—We thank V. Neiveyans, M. Bignon, and C. Soundaramourty for technical assistance. Electron microscopy was done with the help of F. Mongiat. We thank Dr. K. Frenzel for reading the article. We are grateful to Drs. S. L. Milgram (University of North Carolina at Chapel Hill), W. Brown (Cornell University), C. Bucci (Università di Napoli 'Federico II', Italy), M. McNiven (Mayo Clinic, Rochester), and J. W. Creemers (University of Leuven, Belgium) for the gift of antibodies and cDNAs.

REFERENCES

1. Inoue, A., Yanagisawa, M., Kimura, S., Kasuya, Y., Miyauchi, T., Goto, K., and Masaki, T. (1989) *Proc. Natl. Acad. Sci. U. S. A.;* **86,** 2863–2867
2. Rubanyi, G. M., and Polokoff, M. A. (1994) *Pharmacol Rev.;* **46,** 325–415
3. Masaki, T. (1993) *Endocr. Rev.;* **14,** 256–268
4. Kurihara, Y., Kurihara, H., Suzuki, H., Kodama, T., Maemura, K., Nagai, R., Oda, H., Kuwaki, T., Cao, W. H., Kamada, N. *et al.* (1994) *Nature* **368,** 703–710
5. Baynash, A. G., Hosoda, K., Giaid, A., Richardson, J. A., Emoto, N., Hammer, R. E., and Yanagisawa, M. (1994) *Cell* **79,** 1277–1285
6. Hosoda, K., Hammer, R. E., Richardson, J. A., Baynash, A. G., Cheung, J. C., Giaid, A., and Yanagisawa. M. (1994) *Cell* **79,** 1267–1276
7. Clouthier, D. E., Hosoda, K., Richardson, J. A., Williams, S. C., Yanagisawa, H., Kuwaki, T., Kumada, M., Hammer, R. E., and Yanagisawa, M. (1998) *Development* **125,** 813–824
8. Haynes, W. G., and Webb, D. J. (1998) *J. Hypertens.* **16,** 1081–1098
9. Egidy, G., Juillerat-Jeanneret, L., Jeannin, J. F., Korth, P., Bosman, F. T., and Pinet, F. (2000) Am. J. Pathol. **157,** 1863–1874
10. Egidy, G., Baviera, E., Ciuffo, G., Corvol, P., and Pinet, F. (2001) *Hypertension* **38,** 1137–1142
11. Denault, J. B., Claing, A., D'Orleans-Juste, P., Sawamura, T., Kido, T., Masaki, T., and Leduc, R. (1995) *FEBS Lett.* **362,** 276–280
12. Blais, V., Fugere, M., Denault, J. B., Klarskov, K., Day, R., and Leduc, R. (2002) *FEBS Lett.* **524,** 43–48
13. Okada, K., Miyazaki, Y., Takada, J., Matsuyama, K., Yamaki, T., and Yano, M. (1990) *Biochem. Biophys. Res. Commun.* **171,** 1192–1198
14. Xu, D., Emoto, N., Giaid, A., Slaughter, C., Kaw, S., deWit, D., and Yanagisawa, M. (1994) *Cell* **78,** 473–485
15. Harrison, V. J., Barnes, K., Turner, A. J., Wood, E., Corder, R., Vane, J. R. (1995) *Proc. Natl. Acad. Sci. U. S. A.* **92,** 6344–6348
16. Parnot, C., Le Moullec, J. M., Cousin, M. A., Guedin, D., Corvol, P., and Pinet, F. (1997) *Hypertension* **30,** 837–844
17. Levy, N., Gordin, M., Mamluk, R., Yanagisawa, M., Smith, M. F., Hampton,

J. H., and Meidan, R. (2001) *Endocrinology* **142,** 5254–5260
18. Schmidt-Ott, K. M., Tuschick, S., Kirchhoff, F., Verkhratsky, A., Liefeldt, L., Kettenmann, H., and Paul, M. (1998) J. Cardiovasc. Pharmacol. **31,** S364–366
19. Tripiciano, A., Peluso, C., Morena, A. R., Palombi, F., Stefanini, M., Ziparo, E., Yanagisawa, M., and Filippini, A. (1999) *J. Cell Biol.* **145,** 1027–1038
20. Schmidt, M., Kroger, B., Jacob, E., Seulberger, H., Subkowski, T., Otter, R., Meyer, T., Schmalzing, G., and Hillen H. (1994) *FEBS Lett.* **356,** 238–243
21. Takahashi, M., Fukuda, K., Shimada, K., Barnes, K., Turner, A. J., Ikeda, M., Koike, H., Yamamoto, Y., and Tanzawa, K. (1995) *Biochem. J.* **311,** 657–665
22. Shimada, K., Takahashi, M., Turner, A. J., and Tanzawa, K. (1996) *Biochem. J.* **315,** 863–867
23. Shimada, K., Takahashi, M.,and Tanzawa, K. (1994) *J. Biol. Chem.* **269,** 18275–18278
24. Emoto, N., and Yanagisawa, M. (1995) *J. Biol. Chem.* **270,** 15262–15268
25. Yanagisawa, H., Yanagisawa, M., Kapur, R. P., Richardson, J. A., Williams, S. C., Clouthier, D. E., de Wit, D., Emoto, N., and Hammer, R. E. (1998) *Development* **125,** 825–836
26. Yanagisawa, H., Hammer, R. E., Richardson, J. A., Emoto, N., Williams, S. C., Takeda, S., Clouthier, D. E., and Yanagisawa, M. (2000) *J. Clin. Invest.* **105,** 1373–1382
27. Korth, P., Bohle, R. M., Corvol, P., and Pinet, F. (1999) *J. Histochem. Cytochem.* **47,** 447–462
28. Barnes, K., and Turner, A. J. (1997) *Neurochem Res.* **22,** 1033–1040
29. Valdenaire, O., Rohrbacher, E., Mattei, M. G. (1995) *J. Biol. Chem.* **270,** 29794–29798
30. Valdenaire, O., Lepailleur-Enouf, D., Egidy, G., Thouard, A., Barret, A., Vranckx, R., Tougard, C., and Michel, J. B. (1999) *Eur J Biochem.* **264,** 341–349
31. Turner, A. J., Barnes, K., Schweizer, A., and Valdenaire, O. (1998) *Trends Pharmacol Sci.* **19,** 483–486
32. Lorenzo, M. N., Khan, R. Y., Wang, Y., Tai, S. C., Chan, G. C., Cheung, A. H., and Marsden, P. A. (2001) *Biochim. Biophys. Acta* **1522,** 46–52
33. Ikeda, S., Emoto, N., Alimsardjono, H., Yokoyama, M., and Matsuo, M. (2002) *Biochem. Biophys. Res. Commun.* **293,** 421–426
34. Orzechowski, H. D., Richter, C. M., Funke-Kaiser, H., Kroger, B., Schmidt, M., Menzel, S., Bohnemeier, H., and Paul, M. (1997) *J. Mol. Med.* **75,** 512–521
35. Barnes, K., Shimada, K., Takahashi, M., Tanzawa, K., and Turner, A. J. (1996) *J. Cell Sci.* **109,** 919–928
36. Russell, F. D., Skepper, J. N., Davenport, A. P. (1998) *Circ. Res.* **83,** 314–321
37. Schweizer, A., Valdenaire, O., Nelbock, P., Deuschle, U., Dumas Milne Edwards, J. B., Stumpf, J. G., and Loffler, B. M. (1997) *Biochem. J.* **328,** 871–877
38. Azarani, A., Boileau, G., and Crine, P. (1998) *Biochem. J.* **333,** 439–448
39. Valdenaire, O., Barret, A., Schweizer, A., Rohrbacher, E., Mongiat, F., Pinet, F., Corvol, P., and Tougard, C. (1999) *J. Cell Sci.* **112,** 3115–3125
40. Korth, P., Egidy, G., Parnot, C., LeMoullec, J. M., Corvol, P., and Pinet, F. (1997) *FEBS Lett.* **417,** 365–370
41. Schweizer, A., Loffler, B. M., and Rohrer, J. (1999) *Biochem. J.* **340,** 649–656
42. Ades, E. W., Candal, F. J., Swerlick, R. A., George, V. G., Summers, S., Bosse, D. C., and Lawley, T. J. (1992) *J. Invest. Dermatol.* **99,** 683–690
43. Tougard, C., and Picart, R. (1986) *Am. J. Anat.* **175,** 161–177
44. Johnson, G. D., and Ahn, K. (2000) *Anal. Biochem.* **286,** 112–118
45. Molloy, S. S., Thomas, L., Van Slyke, J. K., Stenberg, P. E., and Thomas, G. (1994) *EMBO J.* **13,** 18–33
46. van de Loo, J. W., Creemers, J. W., Bright, N. A., Young, B. D., Roebroek, A. J., Van de Ven, W. J. (1997) *J. Biol. Chem.* **272,** 27116–27123
47. Bucci, C., Thomsen, P., Nicoziani, P., McCarthy, J., and van Deurs, B. (2000) *Mol. Biol. Cell* **11,** 467–480
48. Urrutia, R., Henley, J. R., Cook, T., and McNiven, M. A. (1997) *Proc. Natl. Acad. Sci. U. S. A.* **94,** 377–384
49. Kanyicska, B., Lerant, A., and Freeman, M. E. (1998) *Endocrinology* **139,** 5164–5173
50. Suzuki, H., Yamamoto, T., Kikuyama, S., and Uemura, H. (1997) *Gen. Comp. Endocrinol.* **107,** 12–22
51. Kido, T., Sawamura, T., Hoshikawa, H., D'Orleans-Juste, P., Denault, J. B., Leduc, R., Kimura, J., and Masaki, T. (1997) *Eur J Biochem.* **244,** 520–526
52. Cailler, F., Zappulla, J. P., Boileau, G., and Crine, P. (1999) *Biochem. J.* **341,** 119–126
53. Sandoval, I. V., Bakke, O. (1994) *Trends Cell Biol.* **4,** 292–297
54. Sandoval, I. V., Martinez-Arca, S., Valdueza, J., Palacios, S., and Holman, G. D. (2000) *J. Biol. Chem.* **275,** 39874–39885
55. Emoto, N., Nurhantari, Y., Alimsardjono, H., Xie, J., Yamada, T., Yanagisawa, M., and Matsuo, M. (1999) *J. Biol. Chem.* **274,** 1509–1518
56. Muller, L., Valdenaire, O., Barret, A., Korth, P., Pinet, F., Corvol, P., and Tougard, C. (2000) *J. Cardiovasc. Pharmacol.* **36,** S15–18
57. Savage, P., De Lombaert, S., Shimada, K., Tanzawa, K., and Jeng, A. Y. (1998) *J. Cardiovasc. Pharmacol.* **31,** S16–18
58. Shao, R., Yan, W., and Rockey, D. C. (1999) *J. Biol. Chem.* **274,** 3228–3234
59. Morawietz, H., Talanow, R., Szibor, M., Rueckschloss, U., Schubert, A., Bartling, B., Darmer, D., and Holtz, J. (2000) *J. Physiol.* **525,** 761–770
60. Orzechowski, H. D., Gunther, A., Menzel, S., Zimmermann, A., Funke-Kaiser, H., Real, R., Subkowski, T., Zollmann, F. S., and Paul, M. (2001) *Mol. Pharmacol.* **60,** 1332–1342
61. Barker, S., Khan, N. Q., Wood, E. G., and Corder, R. (2001) *Mol. Pharmacol.* **59,** 163–169
62. Mandel, R., Ryser, H. J., Ghani, F., Wu, M., and Peak, D. (1993) *Proc. Natl. Acad. Sci. U. S. A.* **90,** 4112–4116
63. Terada, K., Manchikalapudi, P., Noiva, R., Jauregui, H. O., Stockert, R. J., and Schilsky, M. L. (1995) *J. Biol. Chem.* **270,** 20410–20416
64. Couet, J., de Bernard, S., Loosfelt, H., Saunier, B., Milgrom, E., and Misrahi, M. (1996) *Biochemistry* **35,** 14800–14805
65. Burgess, J. K., Hotchkiss, K. A., Suter, C., Dudman, N. P., Szollosi, J., Chesterman, C. N., Chong, B. H., and Hogg, P. J. (2000) *J. Biol. Chem.* **275,** 9758–9766